

Multiphase manganese oxides with micron cage structure as high-performance cathode material for AZIBs



Tingting Li, Ruisong Guo*, Leichao Meng, Xiaohong Sun, Yang Li

Key Laboratory of Advanced Ceramics and Machining Technology of Ministry of Education, School of Materials Science and Engineering, Tianjin University, Tianjin, 300072, China. (*rsguo@tju.edu.cn)

Introduction

- Mn_3O_4 has good tolerance to long cycles and prevents agglomeration of $\delta\text{-MnO}_2$.
- The porous structure has a high specific surface area and abundant interior space.
- Micron cage structure shortens $\text{Zn}^{2+}/\text{e}^-$ transport paths.
- The heterostructure and N-doping improve the conductivity of Mn-based materials.
- $\text{N-Mn}_3\text{O}_4/\text{MnO}$ outputs a capacity of 127.7 mAh g^{-1} at 10 A g^{-1} for 2500 cycles.

Results

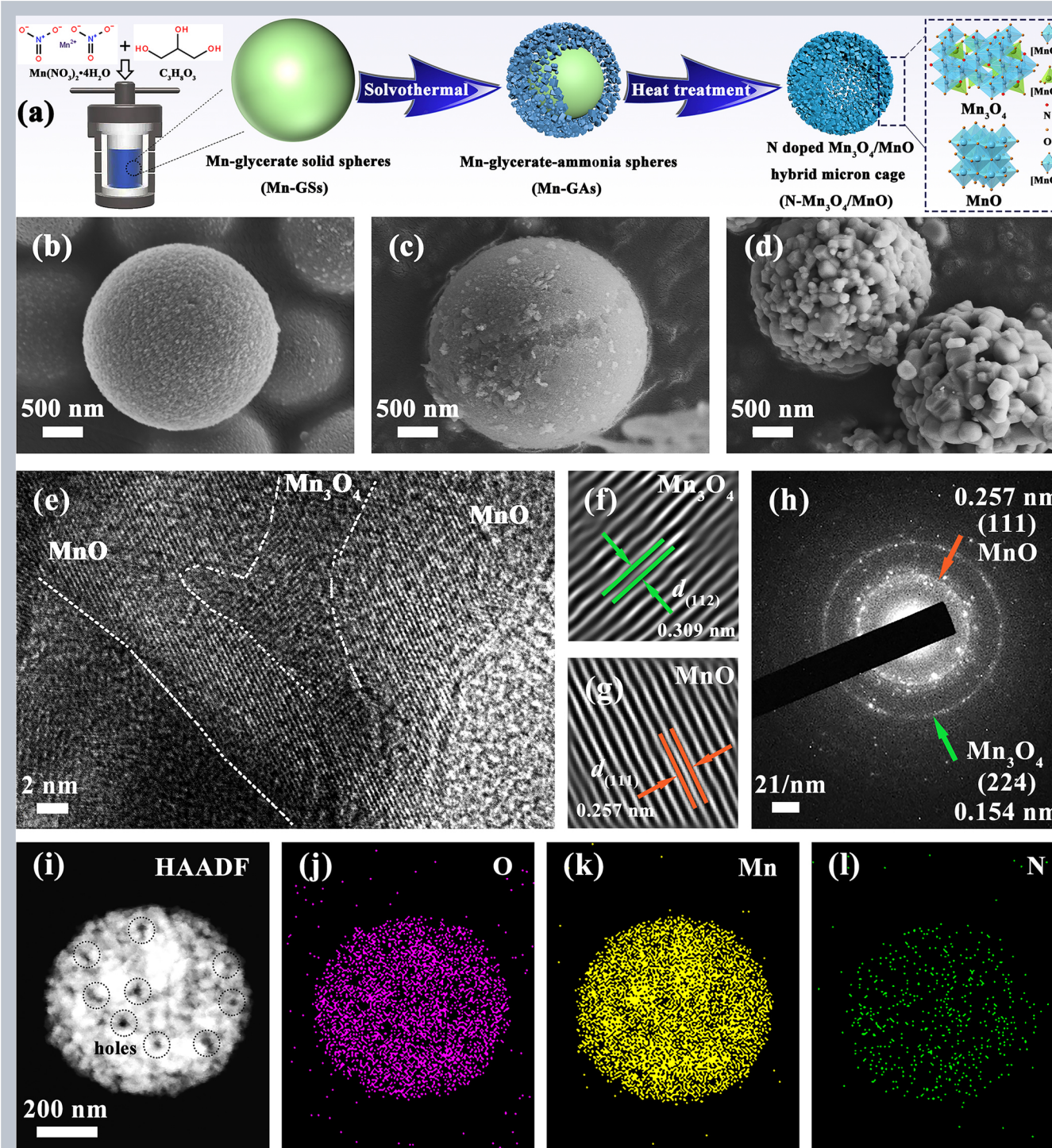


Fig. 1 Schematic illustration of synthesis of the $\text{N-Mn}_3\text{O}_4/\text{MnO}$ hybrid (a). FESEM images of the Mn-GS, Mn-GA and $\text{N-Mn}_3\text{O}_4/\text{MnO}$ powders (b-d), and HRTEM image and EDS images of the $\text{N-Mn}_3\text{O}_4/\text{MnO}$ powders (e-l).

Conclusions

The porous structure of micron cage has high specific surface area, abundant interior space, reduced ion-diffusion path and large electrolyte/electrode contact area. The charge storage mechanism of $\text{H}^+/\text{Zn}^{2+}$ co-insertion reaction. $\text{N-Mn}_3\text{O}_4$ phase acts as a stabilizer, which can alleviate the stress caused by both $\text{Zn}^{2+}/\text{H}^+$ insertion into MnO crystal and the great phase transition. The N/C doping increases the diffusion coefficient, inhibits the Jahn-Teller effect of Mn(III), accelerates the charge transfer and improves the conductivity. $\text{N-Mn}_3\text{O}_4/\text{MnO}$ outputs a capacity of 127.7 mAh g^{-1} after cycling for 2500 at 10 A g^{-1} . Therefore, such an energy storage mechanism provides the $\text{N-Mn}_3\text{O}_4/\text{MnO}/\text{Zn}$ batteries with superior rate capability and stable cycling performance as well.

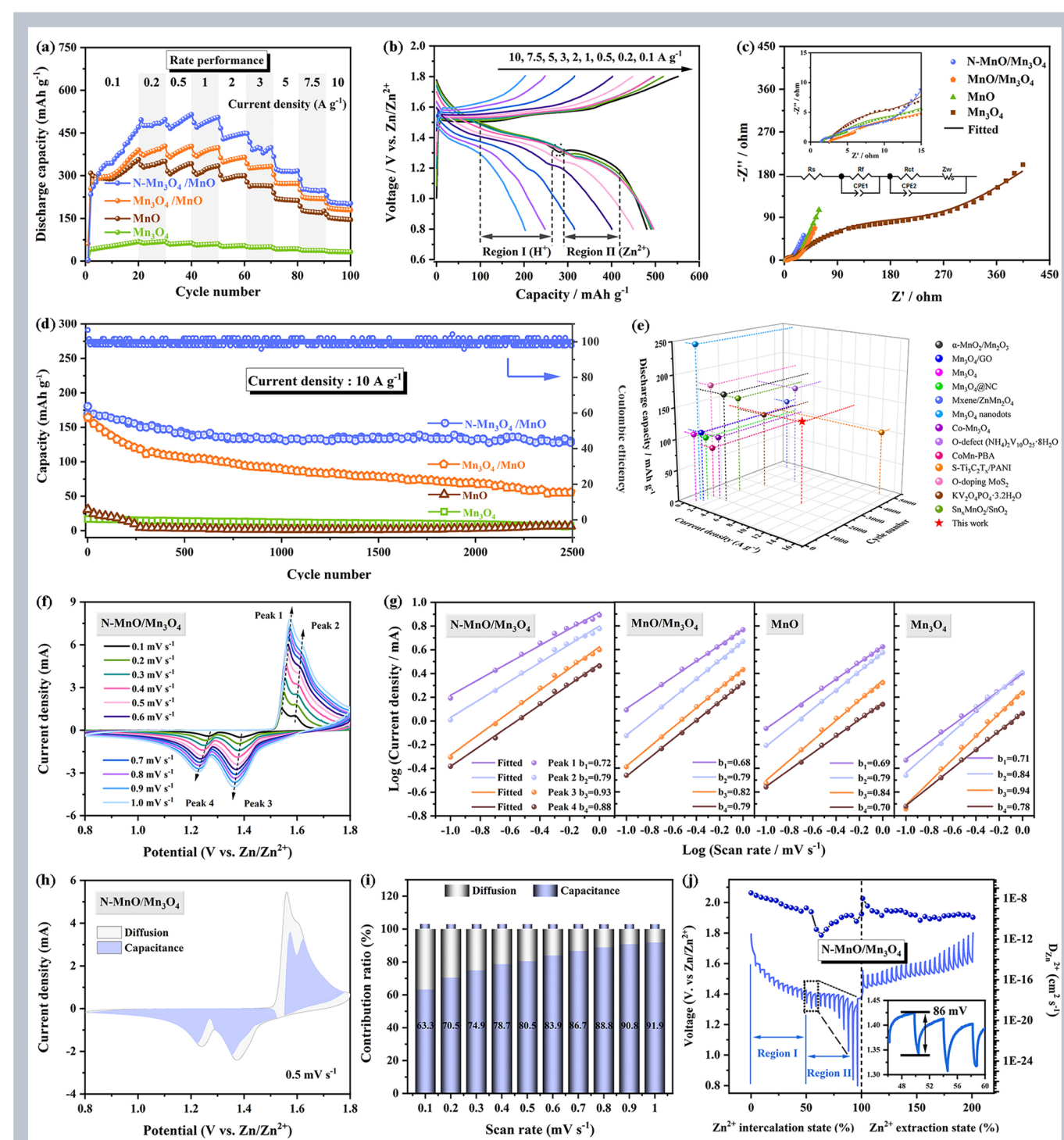


Fig. 2 Rate capability of all cathodes (a), Galvanostatic charge/discharge curves of $\text{N-Mn}_3\text{O}_4/\text{MnO}$ cathode at different current densities (b), EIS patterns of all cathodes before cycle (c), Cyclic performances at 10 A g^{-1} (d), Comparison of cyclic performances of $\text{N-Mn}_3\text{O}_4/\text{MnO}$ cathodes for AZIBs from this work (e), CV curves of $\text{N-Mn}_3\text{O}_4/\text{MnO}$ electrode at various scan rates (f), Corresponding linear fits of the peak currents of all cathodes at various scan rates (g), Capacitive contribution at 0.5 mV s^{-1} (h), Contribution ratio of diffusion/capacitive controlled capacities at various scan rates (i) and GITT voltage profiles of the $\text{N-Mn}_3\text{O}_4/\text{MnO}$ cathodes (j).

Reaction mechanism

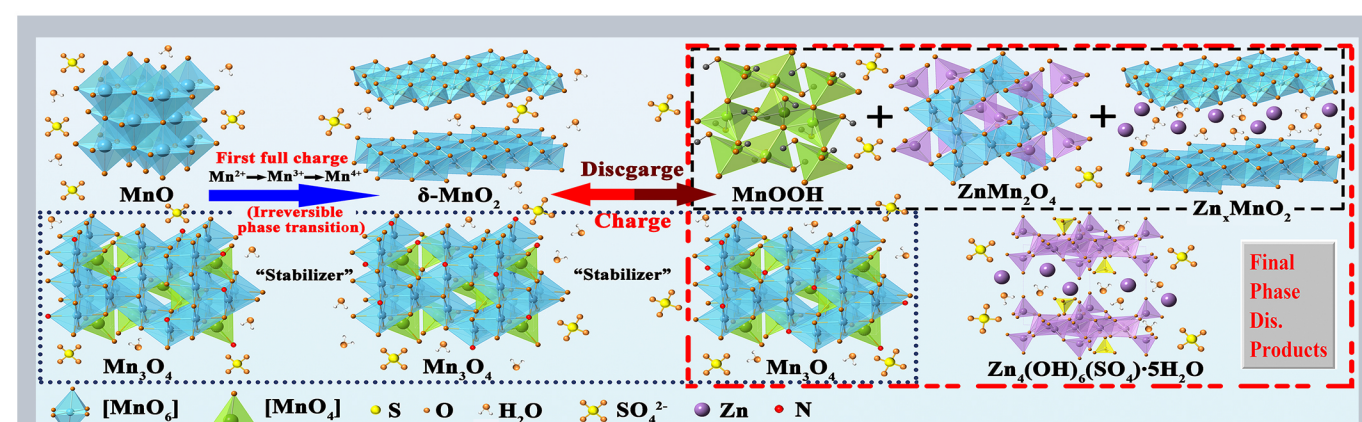


Fig. 3 Schematic illustration of phase transition mechanism